Acta Pharmacologica Sinica (2011) 32: 1276–1284
 1671-4083/11 $32.00
www.nature.com/aps

Original Article

Metabolism of novel anti-HIV agent 3-cyanomethyl-4-methyl-DCK by human liver microsomes and recombinant CYP enzymes

Xiao-mei ZHUANG, Jing-ting DENG, Hua LI[1, *], Wei-li KONG, Jin-xiu RUAN, Lan XIE

The Key Laboratory of Drug Metabolism and Pharmacokinetics, Beijing Institute of Pharmacology and Toxicology, Beijing 100850, China

Aim: To investigate the metabolism of 3-cyanomethyl-4-methyl-DCK (CMDCK), a novel anti-HIV agent, by human liver microsomes (HLMs) and recombinant cytochrome P450 enzymes (CYPs).
Methods: CMDCK was incubated with HLMs or a panel of recombinant cytochrome P450 enzymes including CYP1A2, 2B6, 2C8, 2C9, 2C19, 2D6, 3A4, and 3A5. LC-ion trap mass spectrometry was used to separate and identify CMDCK metabolites. In the experiments with recombinant cytochrome P450 enzymes, specific chemical inhibitors combined with CYP antibodies were used to identify the CYP isoforms involved in CMDCK metabolism.
Results: CMDCK was rapidly and extensively metabolized by HLMs. Its intrinsic hepatic clearance estimated from the *in vitro* data was 19.4 $mL \cdot min^{-1} \cdot kg^{-1}$, which was comparable to the mean human hepatic blood flow rate (20.7 $mL \cdot min^{-1} \cdot kg^{-1}$). The major metabolic pathway of CMDCK was oxidation, and a total of 14 metabolites were detected. CYP3A4 and 3A5 were found to be the principal CYP enzymes responsible for CMDCK metabolism.
Conclusion: CMDCK was metabolized rapidly and extensively in human hepatic microsomes to form a number of oxidative metabolites. CYP3A4 and 3A5 were the predominant enzymes responsible for the oxidation of CMDCK.

Keywords: anti-HIV agent; 3-cyanomethyl-4-methyl-DCK; drug metabolism; enzyme kinetics; liver microsomes; cytochrome P450; CYP3A4; CYP3A5

Acta Pharmacologica Sinica (2011) 32: 1276–1284; doi: 10.1038/aps.2011.91

Introduction

Acquired Immunodeficiency syndrome (AIDS) remains an enormous health threat for humans despite the fact that available chemotherapeutic agents have increased in number and effectiveness in recent years. Currently, 7400 people become infected with human immunodeficiency virus (HIV) every day all over the world. As of 2008, the US Food and Drug Administration (FDA) and European Medicines Agency (EMA) has approved 25 anti-HIV drugs for clinical use, including 5 fixed-dose combinations to deal with the decreased sensitivity of drugs caused by the rapid emergence of drug-resistant mutants[1]. Thus, more effective drugs with novel mechanisms of action or resistance profiles different from those of currently available anti-HIV therapeutics are urgently necessary[2].

3′,4′-Dicamphanoyl-(+)-*cis*-khellactone (DCK) and its analogs are a novel class of non-nucleoside reverse transcriptase inhibitors (NNRTIs) with a novel mechanism. They inhibit DNA-dependent DNA polymerase activity, in contrast to currently marketed NNRTI drugs, which interfere with the RNA polymerase activity of HIV-1 RT[3, 4]. In our prior studies, 3-cyanomethyl-4-methyl-DCK (CMDCK), a DCK analog, was identified as a promising preclinical agent. It exhibited high potency against the replication of both laboratory-adapted HIV strains and primary HIV-1 isolates in a $CD4^+$ T cell line and PBMCs, respectively, as well as moderate efficacy against multidrug-resistant HIV strains (EC_{50}/EC_{90}). Preliminary pharmacokinetic studies indicated that CMDCK has a marginal oral bioavailability (approximately 15%) in rats[5]. Only a very small amount of parent compound was recovered from the urine and bile after oral administration in rats. This result indicated that metabolism was the major elimination pathway of CMDCK in the body. In *in vitro* stability tests, a higher metabolic rate was noted in HLMs than in RLMs (rat liver microsomes) and DLMs (dog liver microsomes), suggesting

* To whom correspondence should be addressed.
E-mail amms_hli@126.com
Received 2011-01-20 Accepted 2011-06-08

that CMDCK may undergo extensive first-pass metabolism in humans.

In the present study, LC-ESI/MS/MS was used to characterize the major oxidative metabolites formed in pooled human liver microsomes (HLMs). The role of CYP enzymes in the biotransformation and metabolic pathways of the candidate drug was investigated using both recombinant human CYP enzymes and HLMs combined with specific CYP antibodies and selective chemical inhibitors.

Materials and methods

Chemicals and materials

CMDCK and an internal standard (chemical structure presented in Figure 1) were synthesized in house with a purity of 98.5% determined by HPLC. Ketoconazole (KET), troleandomycin (TAO), ritonavir (RIT), naphthoflavone, sulfaphenazole, tranylcypromine, quinidine and NADPH were purchased from Sigma-Aldrich (St Louis, MO, USA). Pooled HLMs, human recombinant cytochrome P450 enzymes (CYP1A2, CYP2B6, CYP2C8, CYP2C9, CYP2C19, CYP2D6, CYP3A4, and CYP3A5) with reductase and anti-human CYP2D6 and CYP3A4 antibodies were purchased from BD Gentest Corporation (Woburn, MA, USA). Unless specified, all other reagents and solvents were the highest purity available and were purchased from Sigma-Aldrich Chemical Co (St Louis, USA). All buffers and reagents were prepared with high-purity water (Milli-Q; Millipore, Bedford, MA, USA).

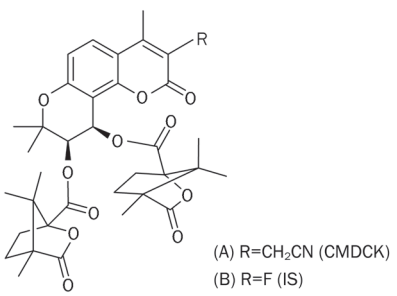

Figure 1. Chemical structures of (A) 3-cyanomethyl-DCK (CMDCK) and (B) IS.

Identification of CMDCK metabolites in HLMs

The incubation mixtures contained CMDCK (10 μmol/L), pooled HLMs (1 mg/mL), and NADPH (1 mmol/L) in 100 mmol/L sodium phosphate buffer (pH 7.4). The reactions were started by the addition of an NADPH solution after a 5-min preincubation. Incubations were carried out at 37 °C for 60 min and stopped by adding an equal volume of ice-cold methanol/acetonitrile (1/4, *v/v*). The suspension was centrifuged (20 000×*g*, 10 min), and an aliquot (20 μL) of the supernatant was analyzed directly by HPLC/PDA for metabolite screening and by LC/MS/MS for structural elucidation.

CYP phenotyping of CMDCK with recombinant CYP enzymes

CMDCK (4 μmol/L, unless otherwise indicated, dissolved in incubation buffer) was incubated separately in sodium phosphate buffer (100 mmol/L, pH 7.4) containing recombinant CYP1A2, CYP2B6, CYP2C8, CYP2C9, CYP2C19, CYP2D6, CYP3A4, and CYP3A5 coexpressed with cytochrome b5 in a final volume of 200 μL. Supersomes were used at P450 protein concentrations of 25 nmol/L. After preincubation for 5 min at 37 °C, the reaction was initiated by the addition of NADPH (1.0 mmol/L) and was terminated at 30 min by adding 200 μL of cold acetonitrile. Subsequently, 400 μL of IS solution (3.8 μmol/L, dissolved in acetonitrile) was added to the samples, followed by centrifugation (10 min, 20 000×*g*, 4 °C). An aliquot of 100 μL of supernatant was taken for ESI-LC-MS analysis as described below. Control microsomes prepared from insect cells infected with wild-type baculovirus were used as negative controls for native enzyme activities. The incubations were performed in triplicate.

Chemical inhibition and immunoinhibition studies in HLMs

For chemical inhibition studies, CMDCK (4 μmol/L) was incubated with pooled HLMs in the absence (control) and presence of selective CYP chemical inhibitors for 30 min. The inhibitors used were naphthoflavone (50 μmol/L) for CYP1A2, sulfaphenazole (10 μmol/L) for CYP2C9, tranylcypromine (50 μmol/L) for CYP2C19, quinidine (10 μmol/L) for CYP2D6, and KTZ (1, 2, or 5 μmol/L), RIT (1, 2, or 5 μmol/L), and TAO (100, 250, or 500 μmol/L) for CYP3A4. TAO, a time-dependent-mechanism–based inhibitor of CYP3A4, was preincubated at 37 °C for 15 min with HLMs and NADPH before the substrate was added to start the reaction. Control incubations were carried out in appropriate solvents (incubation buffer or 0.1% DMSO) that contained no inhibitors.

In immunoinhibition studies, the concentrations of the CYP2D6 and CYP3A4 antibodies used in the experiments were in accordance with the manufacturers' instructions. The incubation conditions were from the same as those used for the kinetic analyses, except that the HLMs and antibodies were preincubated for 15 min on ice before addition of the remaining incubation constituents. Control incubations were similarly preincubated but did not contain antibodies. Experiments were performed in triplicate.

Kinetics studies using HLMs and recombinant CYP3A4 enzymes

Preliminary experiments (data not shown) were performed to determine the optimal incubation conditions in HLMs to ensure linearity with respect to the microsomal protein concentration and the incubation time. A typical incubation contained 0.5 mg/mL of HLMs, 4 μmol/L of CMDCK, 1 mmol/L of NADPH, 5 mmol/L of $MgCl_2$, and 100 mmol/L of sodium phosphate buffer (pH 7.4) in a final volume of 200 μL. Incubation reactions were started and stopped as described above. The supernatant was directly analyzed by ESI-LC-MS as described below. Negative control incubations were performed by omitting NADPH.

Kinetic parameters (apparent K_m and V_{max}) in the pooled HLMs (0.5 mg/mL) and CYP3A4 (25 nmol/L) samples were determined with a series of CMDCK concentrations ranging

from 0.25 to 25 μmol/L. All incubations were performed in duplicate.

Instrumental analysis

A Thermo Finnigan Surveyor HPLC and a tandem Thermo Finnigan LCQ Ion Trap Mass Spectrometer (ITMS) equipped with an auto-sampler, a PDA detector and a Thermo Kromasil C18 analytical column (3 mm×50 mm id, 5 μm) were used for metabolite identification. A linear gradient elution was performed with the mobile phase consisting of 0.1% aqueous formic acid solution (A) and methanol (B). The gradient began with 20% B, increased linearly to 50% B in the first 4 min, then 70% B in the next 13 min, and back to the initial composition in 2 min, followed by 2 min to re-equilibrate the column. The ITMS with an electrospray ionization (ESI) source, was operated in a positive ionization mode. The operating conditions were as follows: spay voltage of 4.5 kV, capillary temperature of 225 °C, capillary voltage of 20 V, sheath gas of 40 arbitrary units, and collision energy of 50 eV. Ion trap full scan analyses were conducted from *m/z* 500 to 800.

The quantitative analysis of CMDCK was carried out using an Agilent Single Quadrupole Mass Spectrometer (Agilent, Palo Alto, CA, USA) attached to an Agilent 1100 HPLC. ChemStation (Version A 09; Agilent, Palo Alto, CA, USA) was used to control the operation of these instruments and acquire the data. CMDCK and its major metabolites were separated on a 2.1 mm×100 mm BetaBasic C18 column (Thermo Electron, USA) with a 55/45 acetonitrile/water mixture containing 0.1% formic acid. The total running time was 17 min at a flow rate of 0.2 mL/min. The MS assay was conducted using the MSDVL electro-spray interface, operating in positive selective ion monitoring (SIM) mode. The detected ions were selected at *m/z* 693 $[(M+NH_4)^+]$ for the quantitative analysis of CMDCK. The ions at 709 $[(M+O+NH_4)^+]$, 725 $[(M+2O+NH_4)^+]$, and 723 $[(M+2O-2H+NH_4)^+]$ were selected to screen mono-oxidized, di-oxidized and carboxylic metabolites, respectively.

Calibration curves and quality control samples were prepared in heat-inactivated human liver microsomal suspensions at the same protein concentration (0.5 mg/mL) used for incubations. The peak area ratios of CMDCK to the internal standard were linear over the range of 0.1–100 μmol/L. The intraday (within batch) accuracy and precision of the LC-MS assay were determined by repeatedly analyzing the spiked microsomal samples (n=3) at three concentration levels (low, medium and high levels) within the calibration range (*ie*, 0.25, 5, or 50 μmol/L). Inter-day data were obtained by analyzing the same set of spiked samples in duplicate over 3 consecutive days.

Data analysis

The elimination half-life ($t_{1/2}$) of CMDCK was calculated as $t_{1/2}$=0.693/k, where k is the slope of the line obtained by linear regression of the natural logarithmic percentage (ln %) of the remaining parent drug CMDCK versus the incubation time (min). Conversion of *in vitro* CL_{int} was done using the following formula[6]:

$$CL_{int} = \frac{0.693}{in\cdot vitro\cdot T_{1/2}} \times \frac{mL\cdot incubation}{mg\cdot microsomes} \times \frac{mg\cdot microsomes}{g\cdot organ} \times \frac{g\cdot organ}{kg\cdot B.W.}$$

where the microsomal yield (mg/g organ)[7] and liver weight (g/kg body weight) were taken from the literature[8, 9].

Apparent K_m and V_{max} constants were determined using a Lineweaver-Burk plot. The values of CYP3A4 were normalized using nominal amounts of CYP3A4 in HLMs[10].

The *in vitro* value was extrapolated to the *in vivo* intrinsic clearance (CL_h, $mL\cdot min^{-1}\cdot kg^{-1}$ body weight) according to the equation[11]:

$$CL_{int} = \frac{Q \times CL_{int}}{Q + CL_{int}}$$

where Q represents organ blood flow. The hepatic blood flow rate for humans used in the calculation of CL was 20 $mL\cdot min^{-1}\cdot kg^{-1}$ [12].

Results

Metabolite profiling and identification

The biotransformation of CMDCK in HLMs was NADPH dependent, and CMDCK depletion was rapid. A typical HPLC-UV chromatogram of CMDCK metabolites in HLMs is presented in Figure 2. In addition to the parent drug, six major peaks corresponding to the metabolites M1 (+O), M4 (+O), M7 (+O-2H), M12 (+2O-2H), M13 (+3O-2H), and M14 (+3O-2H) were observed. Eight minor metabolites, namely M2-M3 (+O), M5, M6 (-$C_{10}H_{12}O_3$), and M8-M11 (+2O), were also detected in HLMs using the selected ion scan mode of the LC-ITMS (Figure 3). All these metabolites were absent from the control samples without NADPH.

The structural elucidation of CMDCK metabolites was based on ITMS mass spectra. Multiple MS involving repeated

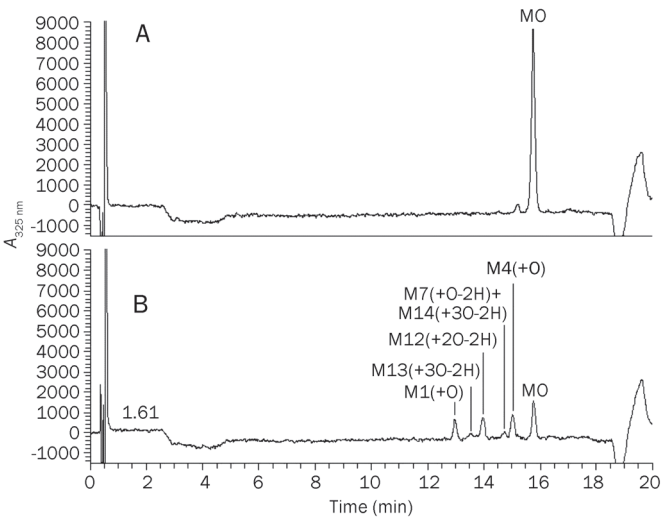

Figure 2. Representative HPLC-UV chromatograms of incubation mixtures of CMDCK with HLMs. (A) Negative control sample without NADPH. (B) Experimental sample with NADPH. CMDCK (4 μmol/L) was incubated with HLMs (0.5 mg/mL) for 30 min at 37 °C in the presence of NADPH (1.0 mmol/L). Metabolites were identified by LC/MS/MS.

trapping and fragmentation of ions was employed to obtain the fragmentation pattern of CMDCK and its metabolites. The ester/ether structure of CMDCK makes it somewhat lipophilic, and it is also lacks basic N-atoms amenable to electronspay ionization (ESI). This compound was first expected to have an unfavorable MS response. During the development of the LC-MS method, however, it was found that this compound has an extraordinarily high MS response in the positive ion mode, with $M+NH_4^+$, $M+Na^+$, and $M+K^+$ adduct ions. The abnormally high ionization potential of these ions is rationalized in Figure 4 (top). The *cis*-conformation of the two camphanic acid ester moieties of CMDCK provides an negative electron cavity that can stabilize a relatively large positive ion such as NH_4^+, Na^+, or K^+, whereas a proton (H^+) might be too small to fit. The MS detector was further tuned for the dominance of the $M+NH_4^+$ ion, as metal ion adducts such as $M+Na^+$ and $M+K^+$ are often not ideal for MS^n-based fragmentation and structural elucidation.

The high MS response of the $M+NH_4^+$ ion provided a solid foundation for detecting and profiling metabolites, including minor ones. The MS^2 spectra of the parent compound with the fragment interpretation are presented in Figure 4 (bottom). The collision energy (CE) in the MS^2 analysis for *m/z*=693 was optimized to 50–60 eV so that the major daughter ion in the MS^2 spectrum, *ie*, *m/z*=478, could undergo further collision-induced dissociation to form abundant smaller fragments that could also be produced in subsequent MS^3 analysis (data not shown). With this approach, MS^2 spectra of CMDCK and its metabolites provided rich fragmentation information for structural elucidation, while MS^3 spectra did not provide further useful information for the structural elucidation of the metabolites.

Three characteristic product ions from the ammonium-adducted molecular ion of CMDCK were observed at *m/z* 478, 298 and 280. The ion *m/z* 478 corresponded to the loss of either the 3′- or the 4′-camphanoyl moiety, and *m/z* 298 was generated from *m/z* 478 by further loss of the remaining camphanoxyl group. The fragment ion *m/z* 280 resulted from the loss of both 3′-and 4′-camphanoyl moieties from the ammonium-adducted molecular ion. Accordingly, a neutral loss of (*m/z* 215) could be observed for either of the two camphanoyl moieties.

The ammonium-adducted molecular ions ($[M+NH_4]^+$) of CMDCK metabolites with changes in observed mass (ΔM) relative to the parent and the spectral data of their product ions together with the fragmentation interpretation are listed in Table 1. The major metabolic pathway of CMDCK in HLMs was oxidation to form mono-oxidized (M1-M4, M7), di-oxidized (M8-M11) and tri-oxidized (M13 and M14) metabolites. The oxidation occurred on one or both the camphanoxyl groups or on the khellactone moiety. Two metabolites (M6 and M7) with one camphanoxyl group missing at either the 3′ or 4′ position as the result of ester hydrolysis were also observed. The proposed metabolic pathway and the putative metabolites of CMDCK in HLMs are presented in Figure 5. Further structural elucidation of the CMDCK metabolites would be required to identify the exact oxidized positions of the metabolites. Such experiments will have to be carried out in the late drug development stage, after standard reference substances of the metabolites are available or after purified metabolites are obtained from *in vitro* or *in vivo* samples and analyzed using other instrumental analytical techniques, such as nuclear magnetic resonance.

Validation of the quantitative LC-MS method

The calibration curves were obtained over the CMDCK concentration range of 0.1–100 μmol/L. The mean regression equation of five replicates on different days was Y=-0.136787+0.00824407X, and the correlation coefficient (r^2) was greater than 0.9947. The LLOQ of 0.1 μmol/L was deter-

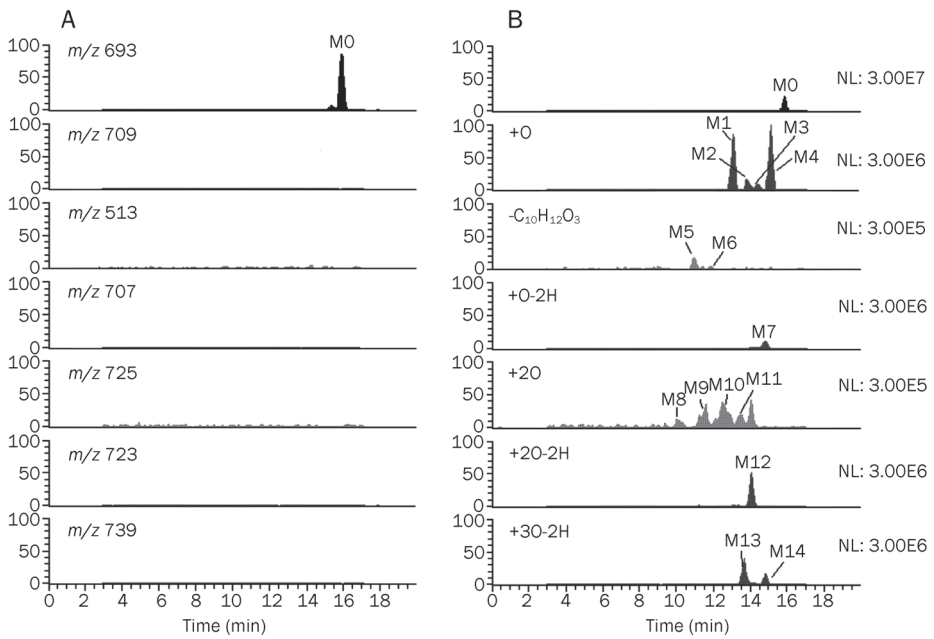

Figure 3. The selected ion chromatograms of CMDCK incubated with HLMs. Control sample without NADPH. (B) Experimental sample with NADPH.

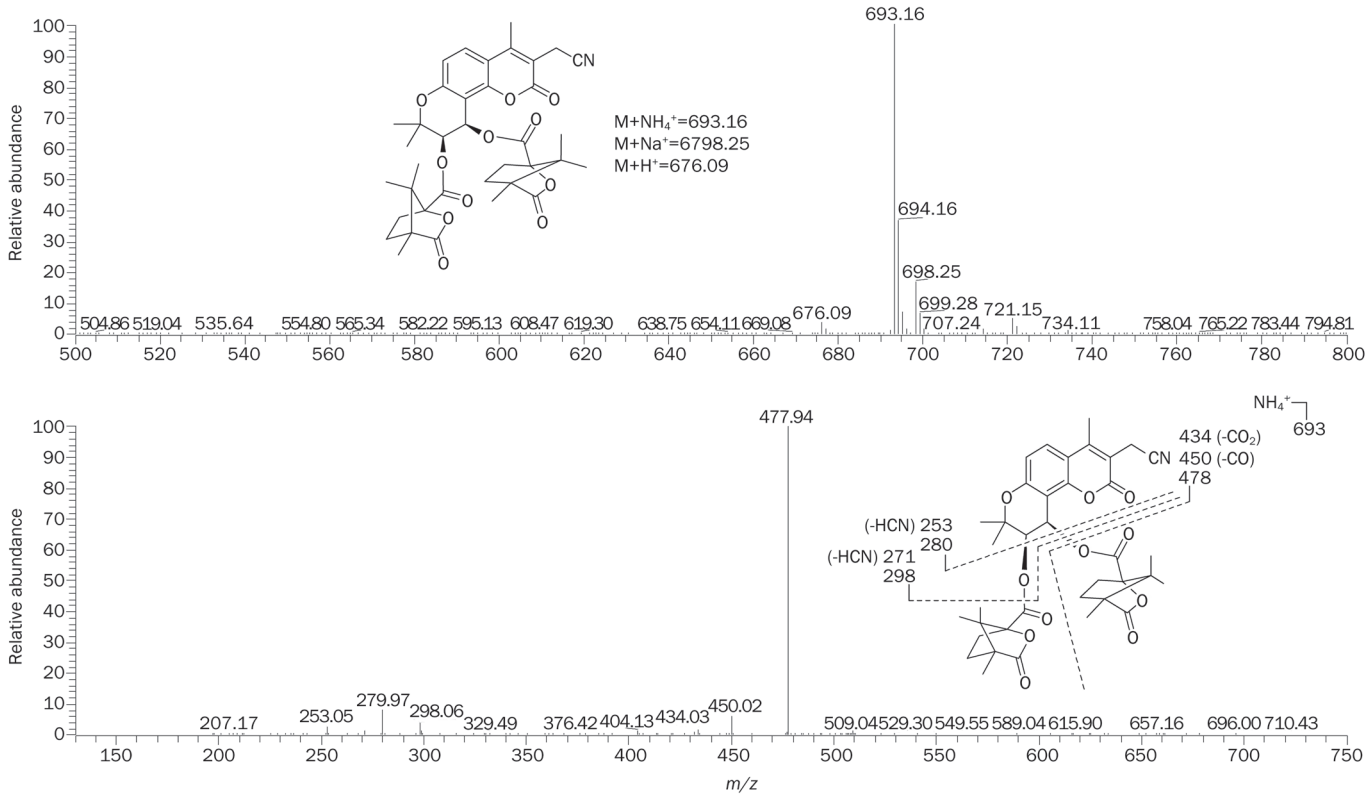

Figure 4. The MS and MS^2 spectra of CMDCK with fragment interpretation.

Table 1. MS fragments and the interpretation of CMDCK metabolites in human liver microsomes.

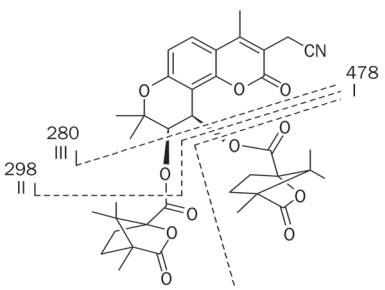

Parent or metabolites	MW	$M+NH_4^+$	Reaction	ΔM	Fragmentations I	II	III
M0	675	693			478	298	280
M1, M2, M4	691	709	+O	16	494	298	280
M3	691	709	+O	16	494	314	296
M5	495	513	$-C_{10}H_{12}O_3$	180		298	
M6	495	513	$-C_{10}H_{12}O_3$	180	478	298	
M7	689	707	+O-2H	14	492	298	280
M8	707	725	+2O	32	494	298	280
M9	707	725	+2O	32	510	314	296
M10	707	725	+2O	32	510	298	280
M11	707	725	+2O	32	494	298	280
M12	705	723	+2O-2H	30	508	298	280
M13, M14	721	739	+3O-2H	46	524	298	280

Fragment ion spectra of ammonium-adducted molecular ions were obtained with a Finnigan LCQ Ion Trap Mass Spectrometer (see Materials and methods).

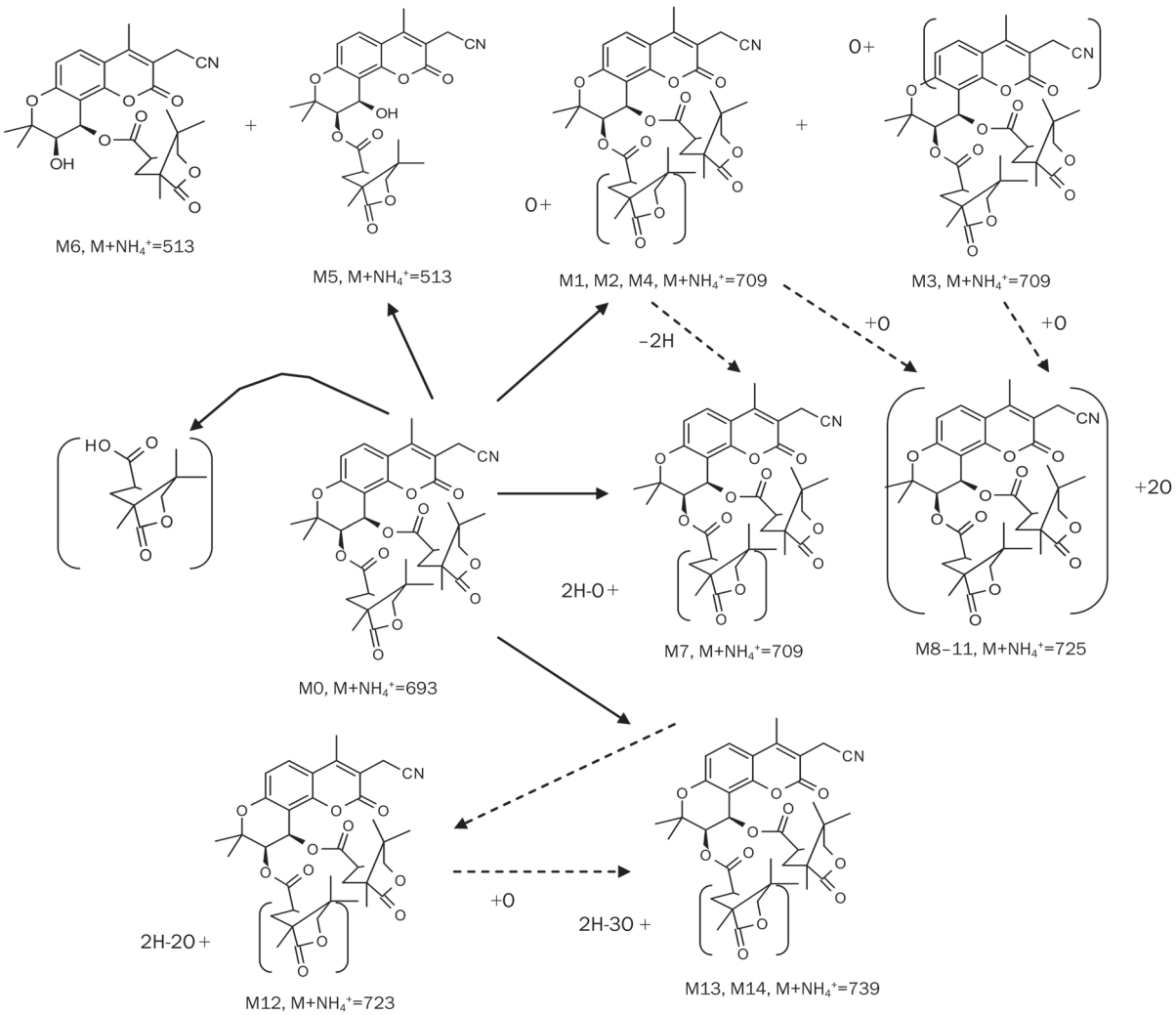

Figure 5. Proposed metabolic pathway of CMDCK in HLMs.

mined based on a signal/noise ratio of 6:1 and on satisfactory precision (RSD<±20%) and accuracy (RE<±20%). The intra- and inter-day precisions and accuracies for CMDCK were assessed based on the analysis of QC samples at three concentration levels (*ie*, 0.25, 5, or 50 μmol/L). The intra-day precisions, expressed as RSD, were all below 11.0%, and the inter-day precisions were <9.0%. The intra-day accuracy ranged from 91.0% to 111.6%, and the inter-day accuracy ranged from 88.6% to 112.4%. All of these values were within the acceptable range (≤15%).

Identification of the CYP isoforms responsible for CMDCK metabolism

Among a panel of eight recombinant human CYP enzymes used for this study, CYP3A4 and 3A5 exhibited a significant catalytic activity related to CMDCK metabolism (Figure 6). All

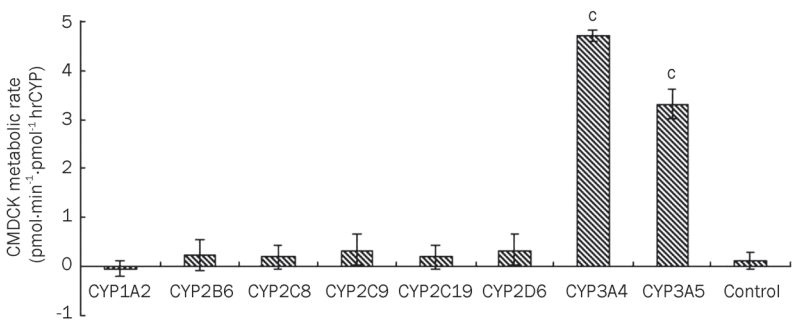

Figure 6. Metabolic rate of CMDCK when incubated with recombinant human CYP isoforms. Incubations were performed using 4 μmol/L of CMDCK, 25 nmol/L of P450 microsomal protein and 1 mmol/L of NADPH for 30 min at 37 °C. Each bar represents the mean of duplicate determinations. A paired *t*-test was used to determine the significant difference in the CMDCK metabolic rate between individual CYP isoforms and the control group. $^{c}P<0.01$ *vs* control.

of the major metabolites observed in HLMs were also detected in the CYP3A4 incubates, whereas no notable metabolic disappearance of the parent was observed in the samples with CYP1A2, 2B6, 2C8, 2C9, 2C19, and 2D6 compared to the control. When the reaction mixtures of these 6 CYP isoenzymes were analyzed using SIM scan mode with the selected ions for major metabolites, no substantial formation of metabolites was observed. CYP3A4 and 3A5 were determined to be the primary CYP isoforms responsible for CMDCK metabolism.

Enzyme kinetics of CMDCK metabolism

The metabolic rates and enzyme kinetic parameters were determined based on the metabolic elimination of the parent compound because currently no standard reference substances for the metabolites are available.

The apparent enzyme kinetic parameters of CMDCK incubated with pooled HLMs and recombinant CYP3A4 are summarized in Table 2. Both the K_m and V_{max} for CMDCK in recombinant CYP3A4 were similar to those in HLMs.

Inhibition of CMDCK metabolism by CYP chemical inhibitors and specific antibodies

The inhibitory effects of the selective chemical inhibitors and immunoinhibitory monoclonal antibodies on CYP3A4 were evaluated at three concentration levels (Table 3) because the substrate specificity and inhibitors for CYP3A4 and CYP3A5 overlapped. The known potent CYP3A4 inhibitors KET and RIT inhibited the formation of the major oxidative metabolites in a concentration-dependent manner. The inhibitory rates at the levels of 1, 2, and 5 μmol/L were 68.3%, 81.9%, and 90.1%, respectively, for KET and 66.7%, 77.5%, and 91.1%, respectively, for RIT. TAO, a mechanism-based CYP3A4 inhibitor, also dose-dependently attenuated CMDCK elimination in liver microsomes with inhibitory rates of 30.8%, 55.9%, and 80.2% at 100, 250, and 500 μmol/L, respectively. However, the effects of the selective inhibitors on CYP1A2, 2C9, 2C19, and 2D6 were found to be either negligible or negative, with inhibitory rates of -0.95%, -0.93%, -1.07%, and 0.45%, respectively.

When CMDCK was incubated with the pooled HLMs in the presence of immunoinhibitory CYP antibodies, only CYP3A4 antibody showed a significant inhibitory effect on CMDCK metabolism, with an inhibitory rate up to 83.9%. The effect of the CYP3A4 antibody was also concentration dependent. In contrast, the CYP2D6 antibody did not show any inhibitory effect on the metabolism of CMDCK. This result provides further evidence demonstrating the predominant role of CYP3A4/3A5 in CMDCK metabolism.

Table 3. Inhibitory effects of selective CYP3A4 inhibitors and specific CYP3A4 antibody on CMDCK metabolism in human liver microsomes (mean±SD, *n*=3).

Inhibitors or monoclonal antibody to CYP3A4	Concentrations (μmol/L or mg/mL protein)	Inhibitory rate (%)
Ketoconazole	1	68.3±9.61
	2	81.9±1.60
	5	90.1±5.20
Ritonavir	1	66.7±1.76
	2	77.5±2.36
	5	91.1±5.47
Troleandomycin	100	30.8±4.98
	250	55.9±3.15
	500	82.0±1.70
MAB-CYP3A4	1	74.9±4.37
	5	83.9±4.03

Discussion

The metabolic stability test of fourteen DCK derivatives indicated that these compounds were all rapidly and extensively metabolized in HLMs under oxidative conditions[13]. CMDCK, a novel DCK analog, was found to have a similar metabolic stability in HLMs. Following the standard metabolic study protocol[14], the enzyme concentrations (0.2–4 mg/mL), reaction times (0–90 min), and substrate concentrations (0.25–50 μmol/L) were optimized. The metabolic kinetic study of CMDCK was subsequently conducted at an enzyme content of 0.5 mg/mL, a substrate concentration of 4 μmol/L and an incubation time of 30 min. As the key parameter for the *in vitro-in vivo* correlation, the intrinsic clearance (CL_{int}) for CMDCK was directly obtained from the *in vitro* $T_{1/2}$[15, 16], based on the widely accepted well-stirred model. The hepatic clearance (CL_h) was then estimated using *in vitro* CL_{int} data (Table 2). It was noted that the CL_h (19.4 mL·min^{-1}·kg^{-1}) of CMDCK was comparative to the mean human hepatic blood flow rate (20.7 mL·min^{-1}·kg^{-1}), which indicated that the liver metabolism of CMDCK would be the predominant elimination pathway *in vivo*.

The CYP reaction phenotyping of CMDCK was conducted using both cDNA-expressing human CYP enzymes and pooled HLMs combined with chemical inhibitors and mono-

Table 2. Kinetic parameters of CMDCK metabolism in reactions with pooled liver (HLMs) and recombinant CYP3A4 enzymes and prediction of the hepatic clearance of CMDCK.

	$t_{1/2}$ min	CL_{int} mL·min^{-1}·kg^{-1}	CL_h mL·min^{-1}·kg^{-1}	Q_h mL·min^{-1}·kg^{-1}	K_m μmol·L^{-1}	V_{max} pmol·min^{-1}·mg^{-1}
HLM	5.62±0.57	311.6±30.8	19.4±0.12	20.7	14.3	1.78
CYP3A4	6.84±1.55	–	–	–	12.1	1.58

clonal antibodies. Among the eight commonly used CYP isoenzymes (CYP1A2, 2B6, 2C8, 2C9, 2C19, 2D6, 3A4, and 3A5), only CYP3A4 and 3A5 showed significant CMDCK metabolism activity. It is well known that the CYP3A subfamily, consisting mainly of CYP3A4 and 3A5 in adults, is responsible for the metabolism of more than half of therapeutic agents that undergo oxidation[17]. CYP3A4 and 3A5 share most of the same substrates[18], and *in vitro* investigations have indicated that CYP3A5 can be less susceptible to inhibition than CYP3A4. In the present study, CYP3A4 and CYP3A5 were identified to be the principal enzymes involved in CMDCK metabolism in the human liver. Oxidation was the major metabolic pathway of CMDCK. A number of metabolites including 12 oxidative products and 2 hydrolysis metabolites, were identified. The oxidation occurred on either of the two camphanoyl groups or on the khel lactone moiety. The rapid and extensive CMDCK metabolism mediated by CYP3A4 and CYP3A5 might lead to low bioavailability in the human body[19, 20].

In general, a higher conversion rate of a drug candidate *in vitro* is unfavorable because the conversion rate is predictive of higher hepatic clearance *in vivo*, resulting in a significant first pass effect for oral administration[21]. In fact, a number of clinically available anti-HIV agents exhibit significant first-pass hepatic metabolism. This problem was solved by the drug combination regime called HAART (highly active antiretroviral therapy), whose goals were same as those of the treatment of tuberculosis[22]. In this study, significant inhibitory effects on CMDCK metabolism were observed for the potent CYP3A4/3A5 inhibitors ketoconazole, ritonavir and troleandomycin. This result suggested that coadministration of CMDCK with a potent CYP3A inhibitor, such as ritonavir, would enhance its hepatic metabolic stability and subsequently improve its bioavailability in the body. Ritonavir is a protease inhibitor clinically used as an anti-HIV drug. It also widely used as a CYP3A4 inhibitor to boost the effect of other anti-HIV agents for the treatment of AIDS[23]. Some research has indicated that the elevation and prolongation of the plasma levels of some protease inhibitors (such as tipranavir, saquinavir or indinavir) by ritonavir coadministration may produce a composite suppression of HIV viral replication in excess of the sum of that was observed with either agent individually[24, 25]. The effect of ritonavir on CMDCK pharmacokinetics will be further assessed *in vitro* and *in vivo*.

In summary, CMDCK was metabolized rapidly in human hepatic microsomes to form a number of oxidative metabolites. CYP3A4 and CYP3A5 were the predominant enzymes involved in the oxidation of CMDCK.

Acknowledgements

This study was supported by Chinese National Science & Technology Major Special Project on Major New Drug Innovation (2009ZX09102-008) and by a grant from the Beijing Municipal Science and Technology Commission (D0206001040191). We thank Dr Yao-qiu ZHU of MetabQuest Co for his generous assistance with metabolite identification.

Author contribution

Xiao-mei ZHUANG and Hua LI were responsible for the study design, data analysis, and writing of the paper. Xiao-mei ZHUANG, Jing-ting DENG, and Wei-li KONG conducted the experiments. Lan XIE was responsible for the CMDCK project, and she also provided the CMDCK standard. Jin-xiu RUAN was a senior advisor and provided valuable advice.

References

1 De Clercq E. Anti-HIV drugs: 25 compounds approved within 25 years after the discovery of HIV. Int J Antimicrob Agents 2009; 33: 307–20.
2 Kostova I, Raleva S, Genova P, Argirova R. Structure-activity relationships of synthetic coumarins as HIV-1 Inhibitors. Bioinorg Chem Appl 2006; 68274.
3 Huang L, Yuan X, Yu D, Lee KH, Chen CH. Mechanism of action and resistant profile of anti-HIV coumarin derivatives. Virology 2005; 332: 623–8.
4 Xie L, Zhao CH, Zhou T, Chen HF, Fan BT, Che XH, *et al*. Molecular modeling, design, synthesis, and biological evaluation of novel 3′,4′-dicamphanoyl-(+)-*cis*-khellactone (DCK) analogs as potent anti-HIV agents. Bioorg Med Chem 2005; 13: 6435–49.
5 Xie L, Guo HF, Lu H, Zhuang XM, Zhang AM, Wu G, *et al*. Development and preclinical studies of broad-spectrum anti-HIV agent (3′*R*,4′*R*)-3-cyanomethyl-4-methyl-3′,4′-di-*O*-(S)-camphanoyl-(+)-*cis*-khellactone (3-cyanomethyl-4-methyl-DCK). J Med Chem 2008; 51: 7689–96.
6 Obach RS. Prediction of human clearance of twenty-nine drugs from hepatic microsomal intrinsic clearance data: An examination of *in vitro* half-life approach and nonspecific binding to microsomes. Drug Metab Dispos 1999; 27: 1350–9.
7 Houston JB. Utility of *in vitro* drug metabolism data in prediction of *in vivo* metabolic clearance. Biochem Phannacol 1994; 47: 1469–79.
8 Davies B, Morris T. Physiological parameters in laboratory animals and humans. Pharm Res 1993; 10: 1093–5.
9 Gerlowski LE, Jain RK. Physiologically based pharmacokinetic modeling: Principles and applications. J Pham Sci 1983; 72: 1103–27.
10 Rodrigues AD. Integrated cytochrome P450 reaction phenotyping: attempting to bridge the gap between cDNA-expressed cytochromes P450 and native human liver microsomes. Biochem Pharmacol 1999; 57: 465–80.
11 Yamazaki M, Suzuki H, Sugiyama Y. Recent advances in carrier-mediated hepatic uptake and biliary excretion of xenobiotics. Pharm Res 1996; 13: 497–513.
12 Boxenbaum H. Interspecies variation in liver weight, hepatic blood flow, and antipyrine intrinsic clearance: extrapolation of data to benzodiazepines and phenytoin. J Pharmacokinet Biopharm 1980; 8: 165–76.
13 Suzuki M, Li Y, Smith PC, Swenberg JA, Martin DM, Morris-Natschke SL, *et al*. Anti-AIDS agents 65: investigation of the *in vitro* oxidative metabolism of 3′,4′-Di-*O*-(−)-camphanoyl-(+)-*cis*-khellactone derivatives as potent anti-HIV agents. Drug Metab Dispos 2005; 33: 1588–92.
14 Masimirembwa CM, Bredberg U, Andersson TB. Metabolic stability for drug discovery and development: pharmacokinetic and biochemical challenges. Clin Pharmacokinet 2003; 42: 515–28.
15 Obach RS, Baxter JG, Liston TE, Silber BM, Jones BC, MacIntyre F, *et al*. The prediction of human pharmacokinetic parameters from preclinical and *in vitro* metabolism data. J Pharmacol Exp Ther 1997; 283: 46–58.
16 Reddy A, Heimbach T, Freiwald S, Smith D, Winters R, Michael S, *et al*. Validation of a semi-automated human hepatocyte assay for the

determination and prediction of intrinsic clearance in discovery. J Pharm Biomed Anal 2005; 37: 319–26.
17 Wilkinson GR. Drug metabolism and variability among patients in drug response. N Engl J Med 2005; 352: 2211–21.
18 Huang W, Lin YS, McConn DJ 2nd, Calamia JC, Totah RA, Isoherranen N, *et al*. Evidence of significant contribution from CYP3A5 to hepatic drug metabolism. Drug Metab Dispos 2004; 32: 1434–45.
19 Li W, Liu Y, He YQ, Zhang JW, Gao Y, Ge GB, *et al*. Characterization of triptolide hydroxylation by cytochrome P450 in human and rat liver microsomes. Xenobiotica 2008; 38: 1551–65.
20 Kim AR, Lim SJ, Lee BJ. Metabolic inhibition and kinetics of raloxifene by pharmaceutical excipients in human liver microsomes. Int J Pharm 2009; 368: 37–44.
21 Shin HS, Bae SK, Lee MG. Pharmacokinetics of sildenafil after intravenous and oral administration in rats: hepatic and intestinal first-pass effects. Int J Pharm 2006; 320: 64–70.
22 Cahn P, Villacian J, Lazzarin A, Katlama C, Grinsztejn B, Arasteh K, *et al*. Ritonavir-boosted tipranavir demonstrates superior efficacy to ritonavir — boosted protease inhibitors in treatment-experienced HIV-infected patients: 24-week results of the RESIST-2 trial. Clin Infect Dis 2006; 43: 1347–56.
23 MacGregor TR, Sabo JP, Norris SH, Johnson P, Galitz L, McCallister S. Pharmacokinetic characterization of different dose combinations of coadministered tipranavir and ritonavir in healthy volunteers. HIV Clin Trials 2004; 5: 371–82.
24 Li F, Wang L, Guo GL, Ma X. Metabolism-mediated drug interactions associated with ritonavir-boosted tipranavir in mice. Drug Metab Dispos 2010; 38: 871–8.
25 Scott JD. Simplifying the treatment of HIV infection with ritonavir-boosted protease inhibitors in antiretroviral-experienced patients. Am J Health Syst Pharm 2005; 62: 809–15.